

E15-2008-99

EXPERIMENTAL INVESTIGATION  
OF MUON CATALYZED  $t + t$  FUSION

Submitted to «ЖЭТФ»

Богданова Л. Н. и др.

E15-2008-99

Экспериментальное исследование реакции мюонного  $t + t$ -катализа

На мюонном пучке фазотрона ЛЯП ОИЯИ коллаборацией  $\mu$ CF проведено исследование процесса мюонного катализа (МК) в тритии. Проведены измерения с жидкотритиевой мишенью при температуре 22 К и плотности  $\simeq 1,25$  от плотности жидкого водорода (LHD). Получены параметры цикла МК: скорость образования молекулы  $tt\mu$   $\lambda_{tt\mu} = 2,84 (0,32) \text{ мкс}^{-1}$ , скорость реакции синтеза  $tt$   $\lambda_f = 15,6 (2,0) \text{ мкс}^{-1}$  и вероятность прилипания мюона к гелию  $\omega_{tt} = 13,9 (1,5) \%$ . Полученные результаты находятся в согласии с ранее полученными результатами других групп, однако, благодаря уникальному экспериментальному методу, достигнута более высокая точность.

Работа выполнена в Лаборатории ядерных проблем им. В. П. Дзелепова ОИЯИ.

Препринт Объединенного института ядерных исследований. Дубна, 2008

Bogdanova L. N. et al.

E15-2008-99

Experimental Investigation of Muon Catalyzed  $t + t$  Fusion

Muon catalyzed fusion ( $\mu$ CF) process in tritium was studied by the  $\mu$ CF collaboration on the muon beam of the JINR Phasotron. The measurements were carried out with a liquid tritium target at temperature 22 K and density  $\simeq 1.25$  of liquid hydrogen density (LHD). Parameters of the  $\mu$ CF cycle were determined:  $tt\mu$ -muonic molecule formation rate  $\lambda_{tt\mu} = 2.84 (0.32) \mu\text{s}^{-1}$ ,  $tt$  fusion reaction rate  $\lambda_f = 15.6 (2.0) \mu\text{s}^{-1}$  and probability of muon sticking to helium  $\omega_{tt} = 13.9 (1.5) \%$ . The results agree with those ones earlier obtained by other groups, however, better accuracy was achieved due to our unique experimental method.

The investigation has been performed at the Dzhelepov Laboratory of Nuclear Problems, JINR.

Preprint of the Joint Institute for Nuclear Research. Dubna, 2008

L. N. Bogdanova<sup>1</sup>, V. R. Bom<sup>2</sup>, A. M. Demin<sup>3</sup>, D. L. Demin<sup>4</sup>, C. W. E. van Eijk<sup>2</sup>,  
S. V. Filchagin<sup>3</sup>, V. V. Filchenkov<sup>4</sup>, N. N. Grafov<sup>4</sup>, S. K. Grischechkin<sup>3</sup>, K. I. Gritsaj<sup>4</sup>,  
A. D. Konin<sup>4</sup>, A. V. Kuryakin<sup>3</sup>, S. V. Medved'<sup>4</sup>, R. K. Musyaev<sup>3</sup>, A. I. Rudenko<sup>4</sup>,  
D. P. Tumkin<sup>3</sup>, Yu. I. Vinogradov<sup>3</sup>, A. A. Yukhimchuk<sup>3</sup>, S. A. Yukhimchuk<sup>4</sup>,  
V. G. Zinov<sup>4</sup>, S. V. Zlatoustovskii<sup>3</sup>

---

<sup>1</sup>State Scientific Center of Russian Federation, Institute of Theoretical and Experimental Physics, Moscow, Russia

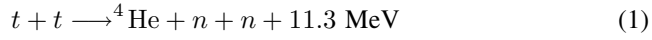
<sup>2</sup>Delft University of Technology, Delft, the Netherlands

<sup>3</sup>Russian Federal Nuclear Center — All-Russian Scientific Research Institute of Experimental Physics, Sarov, Russia

<sup>4</sup>Joint Institute for Nuclear Research, Dzhelapov Laboratory of Nuclear Problems, Dubna, Russia

## 1. INTRODUCTION

Investigation of the muon catalyzed fusion ( $\mu$ CF)  $tt$  reaction



is of a great interest for the complete understanding of the  $\mu$ CF processes in a mixture of hydrogen isotopes and for the study of the nuclear reaction mechanism.

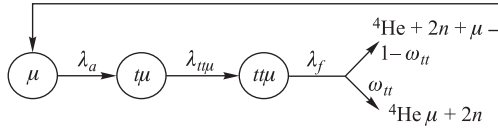


Fig. 1. Diagram of  $\mu$ CF kinetics in tritium

The simplified scheme of  $\mu$ CF kinetics in tritium is shown in Fig. 1. In pure tritium, the stopped muons form  $\mu t$  atoms with a high rate  $\lambda_a$  (about  $10^{10} \mu\text{s}^{-1}$ ). In their collisions with  $T_2$  molecules muonic molecules  $tt\mu$  are produced nonresonantly with the rate  $\lambda_{tt\mu}$  in the rotational-vibrational state  $J = v = 1$ . Fusion from this state competes with muonic molecule de-excitation via the Auger transition to lower levels and with a muon decay. The main de-excitation channel is the  $E0$  Auger transition to the  $(J, v) = (1, 0)$  state, its rate being  $\lambda_{11 \rightarrow 10} \cong 2 \cdot 10^8 \text{ s}^{-1}$  [1]. The de-excitation via the electric dipole transition, which changes the total angular momentum  $J$ , is characterized by the essentially smaller rate, since in the molecules with identical nuclei such a transition necessarily changes the total spin of nuclei and is suppressed. This rate is estimated [1] as  $\lambda_{\Delta J=1} \lesssim 10^4 \text{ s}^{-1}$  that is smaller than the muon decay rate  $\lambda_0 = 0.455 \mu\text{s}^{-1}$ , and the role of such transitions is negligible in cascade de-excitation. Thus fusion reaction in  $tt\mu$  molecule occurs from the states  $J = 1, v = 1, 0$  with a rate  $\lambda_f$ . After fusion a muon is either released with a probability  $(1 - \omega_{tt})$  and can catalyze a new fusion cycle, or is stuck to helium nucleus with a probability  $\omega_{tt}$ .

The  $\mu$ CF  $tt$ -cycle is characterized by the  $tt\mu$  cycling rate  $\lambda_C$ :

$$\lambda_C = \frac{\lambda_f \lambda_{tt\mu}}{\lambda_f + \lambda_{tt\mu}}. \quad (2)$$

The rate of  $tt\mu$ -molecule formation  $\lambda_{tt\mu}$ , the fusion reaction rate  $\lambda_f$  and the coefficient  $\omega_{tt}$  of muon sticking to helium are the main parameters of the  $\mu$ CF  $tt$ -cycle.

A unique possibility of studying low-energy ( $\sim 0.1$  keV)  $p$ -wave  $tt$  fusion (1) is given by the muon catalysis [2]. Till now the  $p$ -wave contribution to  $tt$  fusion cross section has not been determined in difficult collisional experiments at low energies which are complicated by the three-body final state analysis [3]. In  $\mu$ CF experiment one can deduce the  $p$ -wave reaction constant from the experimentally determined  $\mu$ CF fusion rate  $\lambda_f$ . In addition, spectra of fusion neutrons, completed with the data on the muon sticking probability, can distinguish the reaction mechanism. The value of muon sticking coefficient  $\omega_{tt}$  is sensitive to the energy spectrum of  $\alpha$  particle, which somehow reflects particle correlations in the 3-body final state. According to calculations [4],  $\omega_{tt}$  equals to 18, 5 and 10% for  $\alpha n$ ,  $nn$  and no correlations (phase space), respectively.

Observation of  $\alpha n$  or  $nn$  correlations in the  $p$ -wave  $tt$  fusion can shed light on the possible cluster structure of the  $1^-$ -levels in the lightest neutron-rich nucleus  ${}^6\text{He}$ .

However, experimental investigations of the  $\mu$ CF  $tt$  process also face the problem of the continuous neutron energy spectrum of unknown character. It is hard to definitely calculate the neutron detection efficiency  $\epsilon_n$  for using its value in the data analysis.

The way to obtain the  $\mu$ CF parameters without knowing  $\epsilon_n$  was suggested in [5], where the expressions for the total yield  $\eta_{\text{all}}$  (the average of cycles per muon), the yield  $\eta_1$  of the first and the next  $k$ th cycles were firstly obtained. They are

$$\eta_{\text{all}} = \frac{\lambda_{tt\mu}}{\lambda_0 + \lambda_{tt\mu}\omega_{tt}}, \quad \eta_1 = \frac{\lambda_{tt\mu}}{\lambda_0 + \lambda_{tt\mu}}, \quad \eta_k = \eta_1^k (1 - \omega_{tt})^{k-1}.$$

Taking the theoretical values of the  $tt$   $\mu$ CF parameters [4,6,7], we obtain  $\eta_{\text{all}} \simeq 3$  and  $\eta_1 \simeq 0.8$ . Measured yields are  $\eta\epsilon_c$ , where  $\epsilon_c$  is the cycle detection efficiency (detection of at least one neutron from the  $tt$  reaction).

It follows from the analysis [5] that the value of  $\omega_{tt}$  can be directly determined from the ratio of measured yields of the first detected neutrons ( $\eta_1$ ) and the second ones ( $\eta_2$ ):

$$1 - \omega_{tt} = \eta_2 / \eta_1^2. \quad (3)$$

This additional condition makes possible the determination of the  $t + t$   $\mu$ CF parameters without knowing of  $\epsilon_n$ .

However, this method involves large statistical difficulties, because it requires accumulation of  $\sim 10^4$  second neutrons, which is a problem when the value of  $\epsilon_c$  is limited.

So far there were two experiments performed by PSI and RIKEN–RAL groups, where main parameters of the  $\mu$ CF  $tt$ -cycle were determined. The results of these experiments did not completely agree one with another.

In the experiment performed at the muon channel of the PSI meson facility [8] the efficiency was  $\epsilon_n \simeq 1\%$  and the authors could accumulate a few thousand second neutrons and, consequently, obtained the accuracy of about 20–30% for the  $\mu$ CF parameters. Another experiment was carried out by the RIKEN–RAL group [9] at the pulsed beam of the RAL accelerator. The authors could determine the slope of the «slow» component (see below) of the neutron time spectrum. To extract  $\lambda_C$  they made rough determination of neutron yield  $Y_n$  in  $tt$  reaction with 20% accuracy.

The main feature of our experiment is the use of a unique neutron detection system consisting of two high-efficiency neutron detectors placed symmetrically around the target. High  $\epsilon_n \simeq 30\%$  allows high statistics, which is important for the accuracy of the  $\mu$ CF parameters, and, besides, makes possible an independent study of the reaction mechanism by measuring the neutron energy spectrum. The geometry of the installation provides the opportunity to reveal the faint  $n$ – $n$  correlation in the final state of reaction (1).

## 2. EXPERIMENT

The experimental setup is analogous to our previous experiments on  $\mu$ CF [10–12] with some insignificant changes. The experiment was performed at the installation «Triton» mounted on the muon channel [13] of the JINR Phasotron. The experimental setup is schematically shown in Fig. 2. The target (depicted in Fig. 2 as a black circle) was surrounded by a set of detectors.

**2.1. Detectors and Electronics.** Scintillation counters 1–3 detected incoming muons. Cylinder-shaped proportional counters 4 and 5 (analogous to those described in [14]) served to select muon stops in the target (signal  $1 \cdot 2 \cdot 3 \cdot 4 \cdot 5$ ) and to detect electrons from muon decay. Specially designed cylinder-shaped scintillation counters 1-e, 2-e were used to detect  $\mu$ -decay electrons in coincidence with counter 5 (signals  $5 \cdot 1$ -e and  $5 \cdot 2$ -e were considered as a  $\mu$ -decay electron). The full absorption neutron spectrometer (FANS) [15] consisting of two large detectors (ND1 and ND2, each of 12.5 l volume, was the basis of the detection system. It was aimed to detect neutrons from reaction (1).

The timing sequences of the signals from the detectors («oscillograms») were registered by six flash ADC (8 bits  $\times$  2048 samples, 100 Mc/s), depicted in Fig. 2

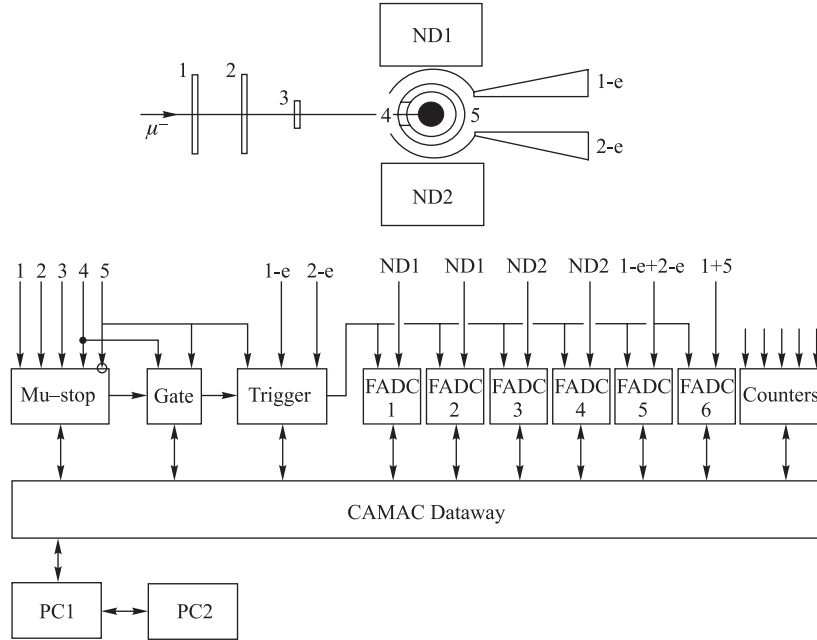


Fig. 2. Experimental lay-out

as FADC 1–6, and were recorded on the PC. An example of the «oscillograms» for one muon measured in the test run is shown in Fig. 3.

A pair of FADC 1,3 was used to read the shortened (30 ns) signals from NDs. With FADC 2,4 the neutron–gamma ( $n - \gamma$ ) separation for the ND signals was realized to discriminate the background. Each ND signal was transformed to the double signal whose parts corresponded to the integral of the «fast» (50 ns) and «slow» (200 ns) components of the ND light pulse. Thus, the signal analysis time was  $\Delta t = 250$  ns. The comparison of the «fast» and «slow» charges made possible to realize the  $n - \gamma$  separation (see Fig. 4). The  $\gamma$ -quantum discrimination efficiency was better than  $10^{-3}$  for energies larger than 100 keV.

Finally, FADC 5,6 registered the signal of the muon stop and the  $\mu$ -decay electron.

The trigger [16] allowed recording of only those events which were connected with the electron detection. During each run the on-line monitoring of data accumulation was conducted.

**2.2. Target and Gas Handling System.** In the experiment the new liquid-tritium target (LTT) with the working volume of  $10 \text{ cm}^3$  [17] was used. LTT was filled with liquid tritium (of amount about  $3.6 \text{ cm}^3$  — about 10 kCi — the

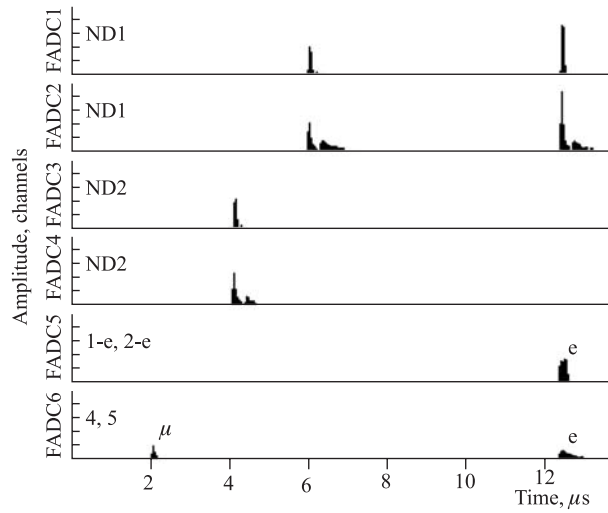


Fig. 3. An example of the «oscillograms» for one muon measured in the test run

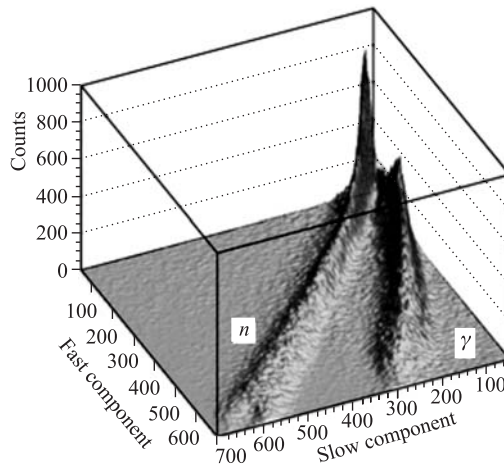


Fig. 4. Three-dimensional plot characterizing the ratio of the amplitudes of fast and slow components of the ND signal

ecological limit for our installation), and kept at temperature of about 22 K and at tritium pressure about 1 atm. To fill the LTT and maintain the needed temperature regime the cryogenic refrigerator was used. A preparation system [18] provided

in-situ purification of tritium gas. Chromatographic method was used to monitor the isotope and molecular composition of the tritium gas [19].

**2.3. Temperature, Pressure and Density Control.** Temperature of liquid tritium was determined by measuring the vapor pressure with tensometric gauges having the accuracy of 0.5%. So, the temperature was determined to be 22.5 K with an accuracy of 0.1 K.

Nuclear density of liquid tritium was determined with the use of cryogenic data on hydrogen isotopes [20]. We obtained the value 1.25 LHD ( $\pm 1\%$ ).

**2.4. Liquid Tritium Purity and  $^3\text{He}$  Accumulation.** The muon transfer from  $t\mu$  atoms to possible impurities influences the measured value of the sticking probability. To reduce this influence for accurate determining of  $\omega_{tt}$ , one should provide the condition

$$\lambda_Z \cdot C_Z \ll \omega_{tt} \cdot \lambda_{tt\mu}, \quad (4)$$

where  $C_Z$  is the fraction of the impurities and  $\lambda_Z$  is the rate of the muon transfer to them. It was necessary to distinguish three sorts of impurities: these with  $Z > 2$ , He and hydrogen isotope admixtures.

**Impurities with  $Z > 2$ .** They were predominately carbon, oxygen and nitrogen. The gas preparation system based on palladium filters [18] provided filling of a target with a gas purified at the level of  $C_Z < 10^{-7}$  of volume parts. The rate of the muon transfer from the  $t\mu$  atom to the admixtures of nuclei with  $Z > 2$  is  $\lambda_Z \sim 10^{11} \text{ s}^{-1}$  [21]. Therefore, condition (4) was satisfied.

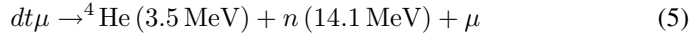
**$^3\text{He}$  admixture.** The tritium preparation system provided the initial  $^3\text{He}$  concentration in tritium  $C_{\text{He}} \simeq 10^{-7}$  before pouring it into a target. However, due to the tritium  $\beta$  decay,  $^3\text{He}$  was accumulated in the target according to relation

$$C_{\text{He}}(\tau) = C_t [1 - \exp(-\lambda_{\text{trit}} \cdot \tau)],$$

where  $\lambda_{\text{trit}} = 1.8 \cdot 10^{-9} \text{ s}^{-1}$  is the tritium decay rate. Hence, the process of the muon transfer from the  $t\mu$ -atom to  $^3\text{He}$  (with the rate  $\lambda_{^3\text{He}} \sim 2 \cdot 10^8 \text{ s}^{-1}$  [22]) could essentially influence the rate of muon loss.

It was shown in experiment [23] that  $^3\text{He}$  in liquid tritium diffuses and goes out to the vapor (gas phase). So there were no problems in liquid tritium purity with respect to the elements with  $Z > 1$  in our experiment. This was confirmed by the coincidence between the observed muon disappearance rate and the muon decay rate (see Subsec. 3.1 below).

**Deuterium and protium admixture in tritium.** In the experiment we used tritium with some initial admixture of other hydrogen isotopes. We clearly observed the presence of deuterium admixture by the «tail» from 14 MeV neutrons from the reaction



in the measured charge spectrum of fusion neutrons (see Fig. 5).

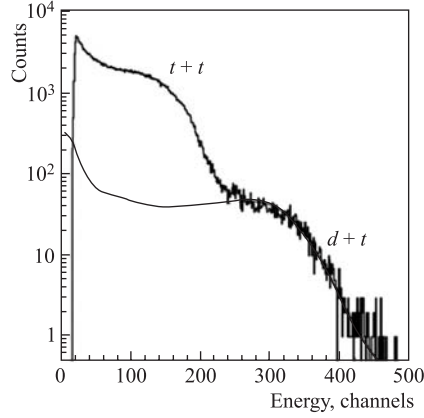


Fig. 5. ND charge spectra measured in the present experiment. Lower line corresponds to the contribution of  $dt$  neutrons. The edge for 14 MeV  $dt$  neutrons corresponds to  $\simeq 400$  channels

The chromatography method [19] used to check the level of hydrogen isotope admixture in tritium showed the presence of less than 1% of deuterium and protium.

### 3. DATA ANALYSIS

The first step in the analysis of the registered events was the separation of neutrons,  $\gamma$ -quanta and  $\mu$ -decay electrons. Then for each exposure we build and analyze the time and charge (deposited energy in a neutron detector) distributions of fusion neutrons. The number of  $\mu$ -decay electrons necessary for normalizing neutron yield was obtained from the analysis of the electron time distribution.

**3.1. Electron Time Spectra.** Time spectra of electrons from muons which stopped and decayed in the target are distorted by the background originating mainly from decay of muons stopping in the target walls. In the run with the empty target we measured the background electron time spectra and obtained the shape of the distribution  $B_{\text{empty}}(t)$ . For the working exposures with tritium-filled target we fitted the electron time spectra taking into account the background spectrum shape:

$$N_e^{\text{tot}}(t) = k \cdot B_{\text{empty}}(t) + A_e \cdot \exp(-\lambda_e t) + F,$$

where  $\lambda_e$  is the muon disappearance rate,  $F$  is an accidental background. In this fit the values  $k$ ,  $A_e$ ,  $\lambda_e$  and  $F$  were the parameters.

The fitted time distribution of decay electrons for the tritium-filled target is shown in Fig. 6. The observed muon disappearance rate  $\lambda_e = 0.456(2) \mu\text{s}^{-1}$

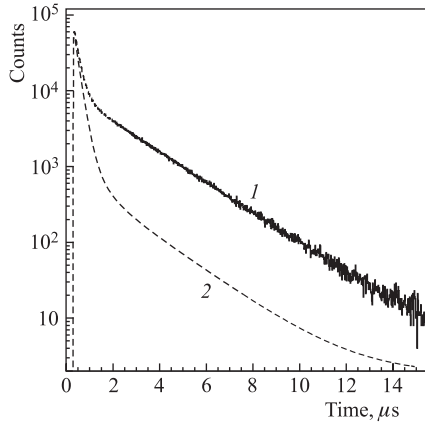


Fig. 6. Electron time distribution. Solid line (1) is the optimum fit for the filled target, dashed line (2) corresponds to electrons from the empty target

found from the fit was in good agreement with the known value for the free muon decay rate  $\lambda_0 = 0.455 \mu\text{s}^{-1}$ . As a result, the number of electrons from muon decay in tritium was obtained:

$$N_e = A_e / (\lambda_e \cdot \Delta\tau) = 972000 \pm 2900,$$

where  $\Delta\tau = 20$  ns is the channel bin. Error in  $N_e$  was about 0.3%. It was determined from the uncertainty in fitting the electron time spectra from the filled (0.2%) and empty (0.2%) target and was mainly defined by total statistics.

### 3.2. Analysis of the Neutron Data.

We analyzed the neutron time distributions to obtain the  $\mu\text{CF}$  parameters. Only the first, second and third detected neutrons were selected for the analysis. Two methods of the analysis, with and without  $n - \gamma$  separation, were applied.

#### Selection of events

1. In the analysis with  $n - \gamma$  separation the events were selected by the shape of ND signal. To exclude pile-up in the time interval  $\Delta t = 250$  ns required for the signal analysis, detected neutrons were specifically selected:

a) The first neutron was accepted if the time between first and second neutrons  $t_{1-2}$  was larger than  $\Delta t$ . If  $t_{1-2} < \Delta t$  we rejected all neutrons caused by this muon.

b) The second neutron was accepted if the time between second and third neutrons  $t_{2-3}$  was larger than  $\Delta t$  and  $t_{1-2} > \Delta t$ . If  $t_{1-2} > \Delta t$  and  $t_{2-3} < \Delta t$  we accepted only the first neutron from all neutrons caused by this muon.

The presence of pile-up was under direct control due to signals on FADC 1, 3. In the present experiment we had found the probability of pile-up within the interval  $\Delta t$  to be

$$\delta \simeq 5 - 6\%.$$

2. Method with  $n - \gamma$  separation required that the analysis is made separately for each ND because of their different parameters. Large neutron detection efficiency of our detectors can lead to a simultaneous registration of two neutrons from the reaction: two neutrons were registered: a) either in the same detector

(one signal) or b) in different NDs (two signals). When we determine the  $\mu$ CF parameters we should deal with the number of  $\mu$ CF cycles, not with the number of neutrons. So in case b) we were forced to take only one neutron in the occasionally chosen ND and to reject another neutron.

3. To reduce the background the time selection criterion

$$t_n + 0.3 \mu s < t_e < t_n + 10 \mu s,$$

was used [24], where  $t_n$  and  $t_e$  are neutron and electron detection times measured from the moment of a muon stop in the target. The low bound discriminated the background due muon stops in the target wall, the upper bound decreased the accidental background caused by false electrons.

**Analytical expressions used for the analysis of neutron time spectra.** The kinetics of the  $\mu$ CF processes in tritium was considered [5] and then, in more detail, in [24], where the Monte-Carlo test calculations were performed, in addition to the analytical consideration. The time distribution of the first detected neutrons (cycles) had the form of the difference of two exponents:

$$dN_1/dt \equiv f_1(t) = A[\exp(-\gamma_1 t) - \exp(-\gamma_2 t)]. \quad (6)$$

The amplitude  $A$  and slopes  $\gamma_1$  and  $\gamma_2$  were determined from the experimental spectrum fit. The  $tt\mu$ -cyclining rate  $\lambda_C$  and other cycle parameters can then be found.

Slopes  $\gamma_1$  and  $\gamma_2$  were expressed through cycle parameters:

$$2\gamma_1 = \lambda_f + \lambda_{tt\mu} + 2\lambda_0 - [(\lambda_f + \lambda_{tt\mu})^2 - 4\alpha \cdot \lambda_f \cdot \lambda_{tt\mu}]^{1/2}, \quad (7)$$

$$2\gamma_2 = \lambda_f + \lambda_{tt\mu} + 2\lambda_0 + [(\lambda_f + \lambda_{tt\mu})^2 - 4\alpha \cdot \lambda_f \cdot \lambda_{tt\mu}]^{1/2}, \quad (8)$$

$$\alpha \equiv \epsilon_c + \omega_{tt}(1 - \epsilon_c).$$

The time distribution of the second detected neutrons was

$$dN_2/dt \equiv f_2(t) = A^2[(\exp(-\gamma_1 t) + \exp(-\gamma_2 t))t + \frac{2}{(\gamma_2 - \gamma_1)}(\exp(-\gamma_1 t) - \exp(-\gamma_2 t))]. \quad (9)$$

It was shown in [24] that the dead time interval ( $\Delta t$ ) does not change the shape of the time distribution for the first neutrons. However, the neutron yields were changed. This led to a modification of expression (3) used for direct determination of  $\omega_{tt}$ . The first neutron yield was

$$\eta'_1 = \eta_1(1 - (1 - \omega_{tt})\delta). \quad (10)$$

The loss in the first neutron yield  $\eta_1$  connected with a dead time selection is 5–6%.

For the second neutrons the corresponding yield was

$$\eta'_2 = \eta_2 \left(1 - \frac{\delta}{\eta_1}\right) (1 - (1 - \omega_{tt})\delta). \quad (11)$$

In this case the loss was more essential and constituted  $\simeq 20\%$ . From Eqs. (3), (10), (11) we have obtained the relation connecting the measured yields  $\eta_1$ ,  $\eta_2$ ,  $\delta$  and  $\omega_{tt}$ :

$$\frac{\eta'_2}{(\eta'_1)^2} = (1 - \omega_{tt}) \frac{1 - \delta/\eta_1}{1 - (1 - \omega_{tt})\delta}. \quad (12)$$

**Analysis with  $n-\gamma$  separation.** Being a means of the background suppression,  $n-\gamma$  analysis was a source of the statistics loss. Besides the necessity to introduce the dead time, we had to remove the events with registration of 4.43-MeV  $\gamma$ s produced in the inelastic threshold process  $n(^{12}\text{C}, \gamma)n'$  (only for high energy ( $> 5$  MeV) neutrons). They distorted the ND signal and must be rejected. It is important that both factors did not lead to ambiguities in the determination of the  $\mu\text{CF}$  parameters, only to a total detection efficiency decrease by  $\simeq 30\%$ .

Experimentally measured time distributions of the first and second detected neutrons are shown in Fig. 7.

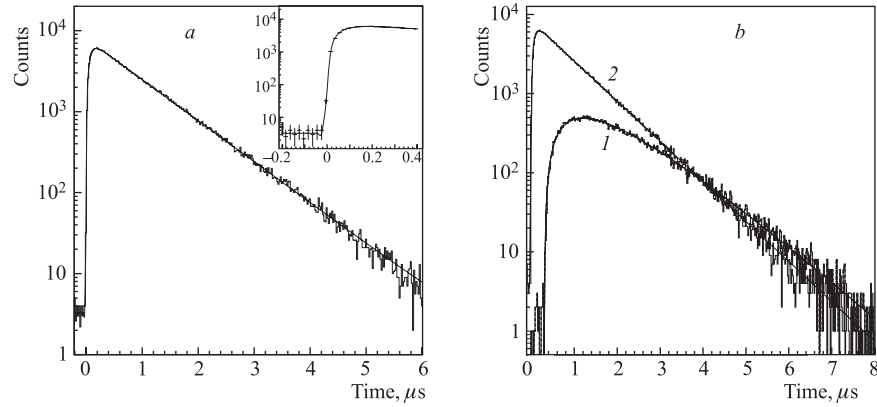


Fig. 7. Time distributions of the first and second detected neutrons with  $n-\gamma$  separation. Lines are the optimum fits. *a*) Time distribution of neutrons from  $dt$  reaction. *b*) Time distributions of the first (1) and second (2) neutrons from  $tt$  reactions

The distribution of the first neutrons was analyzed using Eq. (6). Parameters of this expression (amplitude  $A$  and exponent slopes  $\gamma_{1,2}$ ) were functions of  $\lambda_f$ ,  $\lambda_{tt\mu}$  (formulae (2), (7), (8)). In addition, we measured the numbers of first ( $N_1$ )

and second ( $N_2$ ) detected neutrons and obtained the first ( $\eta_1$ ) and second ( $\eta_2$ ) neutron yields:

$$\eta_1 = N_1/N_e, \quad \eta_2 = N_2/N_e, \quad \eta'_1, \eta'_2.$$

These yields were used for determination of  $\omega_{tt}$  according to expressions (10), (11), (12). Using these yields and values  $A$ ,  $\gamma_{1,2}$  obtained from the fit of the measured time distribution we reconstructed parameters of  $tt$  cycle  $\lambda_f$ ,  $\lambda_{tt\mu}$  and  $\omega_{tt}$ , as well as the neutron detection efficiency  $\epsilon_n$ .

**Influence of  $dt$  neutrons.** A deuterium impurity of about 0.5–1% contained in tritium resulted in the admixture of DT molecules (about  $\sim 0.02$ ) and that of  $D_2$  molecules (about  $\sim 0.0001$ ) in liquid  $T_2$ . The rates of muonic molecule  $dt\mu$  formation on these molecules measured at temperature 22 K were [12]:

$$\lambda_{dt\mu-DT} \simeq 10 \mu\text{s}^{-1}, \quad \lambda_{dt\mu-DD} \simeq 800 \mu\text{s}^{-1}.$$

Formation of  $dt\mu$  molecules becomes essential at such rates and presence of 14-MeV neutrons from the  $dt$  reaction  $dt\mu \rightarrow n + {}^4\text{He} + \mu$  is noticeable in all measured spectra. Amplitude ( $A$ ) and slopes ( $\lambda_{\text{fast}}$ ,  $\lambda_{\text{slow}}$ ) of the first neutron time spectrum, as well as neutron yields ( $\eta_1$  and  $\eta_2$ ) were distorted. Necessary corrections caused by  $dt$  neutrons were introduced in the analysis.

In our work on the muon catalyzed  $dt$  fusion [12] the calculated neutron spectrum was in good agreement with the measured one. We could use the known shape of 14-MeV neutron spectrum in  $dt$  reaction. Analyzing the neutron charge spectrum shown in Fig. 5 we estimated the fraction of  $dt$  neutrons in all distributions. We obtained this contribution as  $\simeq (3.67 \pm 0.27)\%$ . This allowed accurate subtraction of the  $dt$ -neutron spectrum from the time distribution of the first neutrons. Thus we avoided the distortion in the final results of  $\mu\text{CF}$   $tt$  parameters (mainly in  $\lambda_f$ ).

The time distribution of first neutrons for the  $dt$  «tail» did not show «fast» component. It was natural for  $dt$  neutrons, since  $dt$  fusion rate was high (about  $10^{12} \text{ s}^{-1}$ ).

The slope of the  $dt$ -neutron time spectrum exponent was practically the same as the «slow» component for the whole neutron time distribution. So,  $dt$  neutrons did not change the «slow» component ( $\lambda_{\text{slow}}$ ) of  $tt$ -neutron time spectrum.

Since the nuclear density for  $D_2$  and DT molecules was less than 0.01 LHD, the epithermal «spike» in  $dt$  spectrum, appearing when  $t\mu$  atoms pass through the resonances in the muonic molecule formation rates [25], should manifest itself. We observed this spike in the present measurement, like in our previous [26] and PSI [27] experiments.

**Analysis without  $n-\gamma$  separation.** The procedure of the  $n-\gamma$  separation allowed one to reliably discriminate the background but significantly complicated the data interpretation and led to some systematic ambiguities. It was desirable

to find an independent analysis method which would give us the possibility to check the obtained data and verify the results.

Analyzing the  $\gamma$ -background we revealed that it was predominately concentrated just in the time region of a muon stop. So, we decided to make also an analysis *without  $n$ - $\gamma$  separation*. Treating the time of the first neutron as the time of a muon stop in the target, the second neutron as the first and the third one as the second, we plotted the distributions of time difference between second-first and third-first neutrons without  $n$ - $\gamma$  separation. For this distributions we obtained numbers of neutrons  $N_{2-1}$  and  $N_{3-1}$ . The background turned out to be small enough in this case (only a few percent) and it could be easily determined and subtracted. Corresponding measured distributions are shown in Fig. 8.

This method was rather simple and suitable but led to the noticeable decrease of the neutron statistics. For the method with  $n$ - $\gamma$  separation the statistics losses were relatively small ( $\simeq 30\%$ ). For the second method the statistics losses appeared to be larger:  $1 - \eta_1 \simeq 0.6-0.7$ .

To essentially (two times) increase the statistics we performed the combined analysis for both NDs considering them as one detector. So we have succeeded in getting approximately equal statistical power for both analysis methods. The advantage of the combined method was that it allowed both simultaneous detection of two neutrons and, so, to correct  $n$ - $\gamma$  analysis.

The analysis procedure and consideration of  $dt$ -background were analogous to the previous approach. Naturally, expression (3) instead of (10)–(12) was used for  $\omega_{tt}$  determination. The time distributions of first and second neutrons are shown in Fig. 8 together with best fit functions (6) and (9).

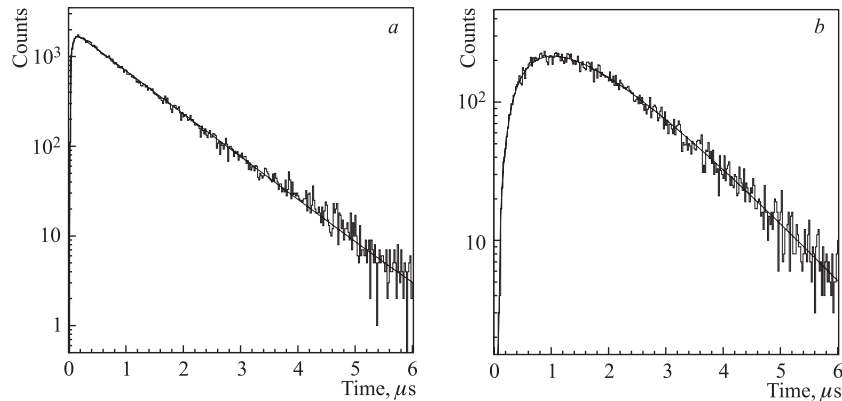


Fig. 8. Time distributions of the second neutrons with respect to the first ones (a) and of the third neutrons relative to the second ones (b). Curves are the fitting functions (6) and (9), respectively, with the optimum parameters

**Results for the main  $tt$   $\mu$ CF parameters.** The main  $\mu$ CF parameters ( $\lambda_f$ ,  $\lambda_{tt\mu}$  and  $\omega_{tt}$ ) obtained by two methods are presented in Table 1. The errors include both statistical and systematic uncertainties. Statistical errors in  $\lambda_f$  and  $\lambda_{tt\mu}$  were determined by the total number of events and the character of the fitting functions. Statistical error in  $\omega_{tt}$  was combined from the uncertainties of the components ( $N_e$ ,  $N_1^2$  and  $N_2$ ) of the ratio  $\eta_2/\eta_1^2$  (2).

The main sources of systematic errors were:

a) uncertainty 1.3% in the value of tritium density was included in the total error for  $\lambda_{tt\mu}$ ,

b) uncertainty 2.1% was due to nonexact knowledge of the deuterium impurity and was included in the error for  $\omega_{tt}$ .

It is seen from Table 1 that both methods give the same result within 15%. This enables assigning the combined values as final results.

**Table 1.  $\mu$ CF parameters of the  $tt$  cycle determined in the present experiment by two analysis methods**

Value	With $n-\gamma$	Without $n-\gamma$	Combined
$\lambda_{tt\mu}$ , $10^6\text{s}^{-1}$	$2.96 \pm 0.32$	$2.56 \pm 0.33$	$2.84 \pm 0.32$
$\lambda_f$ $10^6\text{s}^{-1}$	$15.2 \pm 2.0$	$15.9 \pm 2.1$	$15.6 \pm 2.0$
$\omega_{tt}$ , %	$13.2 \pm 1.5$	$14.6 \pm 1.7$	$13.9 \pm 1.5$

#### 4. DISCUSSION AND CONCLUSION

The experimental data on the main  $tt$   $\mu$ CF parameters ( $tt\mu$ -molecule formation rate  $\lambda_{tt\mu}$ , fusion rate  $\lambda_f$  and sticking probability  $\omega_{tt}$ ) are summarized in Table 2 in comparison with the theoretical predictions.

Results of all experiments show principal agreement with the theoretical predictions. In our experiment the accuracy of the  $tt\mu$ - molecule formation rate was improved by a factor of 2, and the value of  $\lambda_{tt\mu}$  is close to the theoretical one. Our fusion rate  $\lambda_f$  agrees with PSI result [8] and is somewhat larger than the estimate cited in [28], based on the in-flight data [3]. The other theoretical estimate [29] is a few times larger than the observed one.

Our value of the sticking probability  $\omega_{tt}$  agrees with the PSI result. Twice improved accuracy favors the theoretical value obtained with the assumption of  $\alpha-n$  correlation in the final state of reaction (1). Our value of the cycling rate  $\lambda_C = 2.4\mu\text{s}^{-1}$  agrees with that obtained in [9].

In both experimental works [8,9] the evidence for the  $\alpha-n$  correlation was obtained by comparison of the measured recoil proton spectrum of the neutron detector with the one simulated assuming the absence of any final-state correlations.

**Table 2. Parameters of the  $tt \mu\text{CF}$**

Parameter	Source	Ref.	Value
$\lambda_{tt\mu}$ , ( $10^6 \text{ s}^{-1}$ )	PSI experiment	[8]	$1.8 \pm 0.6$
	RIKEN-RAL experiment	[9]	$2.4 \pm 0.6$
	Present experiment		$2.84 \pm 0.32$
	Theory	[6]	2.96
	Theory	[7]	2.64
$\lambda_f$ , ( $10^6 \text{ s}^{-1}$ )	PSI experiment	[8]	$15 \pm 2$
	RIKEN-RAL experiment	[9]	no
	Present experiment		$15.6 \pm 2.0$
	Theory	[28]	13
$\omega_{tt}$ , %	PSI experiment	[8]	$14 \pm 3$
	RIKEN-RAL experiment	[9]	$8.7 \pm 1.9$
	Present experiment		$13.9 \pm 1.5$
	Theory	[28]	14

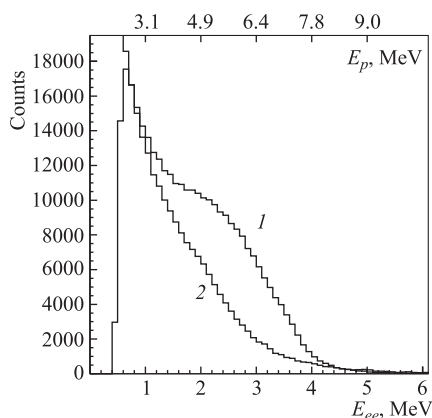


Fig. 9. 1 — Neutron energy spectrum measured in the experiment. 2 — Calculated neutron energy distribution for phase space

Conditions of high efficiency of neutron registration made it possible to obtain main reaction parameters with higher accuracy compared to the earlier experiments.

**Acknowledgments.** The authors are grateful to Prof. L.I.Ponomarev for the stimulating discussions. The work was supported by Ministry of Atomic Energy of RF (contract No. 6.25.19.19.99.969) and by Ministry of Science and Technology of RF (state contract No. 103-7(00)-II). The work has been granted with RFBR (No. 98-02-16351).

This is supported by the neutron spectrum shape obtained in our measurement (Fig.9). The neutron energy spectrum highlights the features of the reaction mechanism:  $n-n$  correlation would result in a concentration of the events in the region  $E_{n1} = E_{n2} = 3.8 \text{ MeV}$  ( $E_{n1}, E_{n2}$  are neutron energies), for  $\alpha-n$  correlation the events are grouped near  $E_{n1} \simeq 9.3 \text{ MeV}$  and  $E_{n2} \simeq 0.5 \text{ MeV}$  (in a simplified consideration) [2]. More detailed analysis of the  $t + t$  reaction mechanism is in progress. Besides, it would be desirable to make the correct calculations of  $\lambda_f$ .

Measurements of the  $\mu\text{CF } tt$  reaction were performed with the use of unique method (FANS, FADC) for the

## REFERENCES

1. *Zeldovich Ya. B., Gershtein S. S.* // Usp. Fiz. Nauk. 1960. V. 71. P. 581.
2. *Bogdanova L. N., Filchenkov V. V.* // Hyp. Int. 2001. V. 138. P. 321.
3. *Serov V. I., Abramovich S. N., Morkin L. A.* // Sov. Phys. At. En. 1977. V. 42. P. 59;  
*Agnew H. M. et al.* // Phys. Rev. 1952. V. 84. P. 862.
4. *Gershtein S. S. et al.* // JETP 1981. V. 53. P. 872.
5. *Filchenkov V. V., Somov L. N., Zinov V. G.* // Nucl. Instr. Meth. 1984. V. 228. P. 174;  
JINR Preprint P15-82-566. Dubna, 1982.
6. *Ponomarev L. I., Faifman M. P.* // Zh. Eksp. Teor. Fiz. 1976. V. 71. P. 1689 (Sov. Phys. JETP. 1976. V. 44. P. 886).
7. *Faifman M. P.* // Muon Cat. Fusion. 1989. V. 4. P. 341.
8. *Breunlich W. H. et al.* // Muon Cat. Fusion. 1987. V. 1. P. 121.
9. *Matsuzaki T. et al.* // Hyp. Int. 1999. V. 118. P. 229;  
*Matsuzaki T. et al.* // Hyp. Int. 2001. V. 138. P. 295;  
*Matsuzaki T. et al.* // Phys. Lett. B. 2003. V. 557. P. 176.
10. *Averin Yu. P. et al.* // Hyp. Int. 1998. V. 118. P. 111.
11. *Bom V. R. et al.* // Hyp. Int. 2001. V. 138. P. 313.
12. *Bom V. R. et al.* // Zh. Eksp. Teor. Fiz. 2005. V. 127. P. 752 (Sov. Phys. JETP. 2005. V. 100. P. 663).
13. *Demianov A. V. et al.* JINR Commun. P9-93-374. Dubna, 1993.
14. *Konin A. D.* JINR Commun. P13-82-634. Dubna, 1982.
15. *Dzhelepov V. P. et al.* // Nucl. Instr. Meth. A. 1988. V. 269. P. 634;  
*Filchenkov V. V., Konin A. D., Zinov V. G.* // Nucl. Instr. Meth. A. 1986. V. 245. P. 490;  
*Baranov V. A. et al.* // Nucl. Instr. Meth. A. 1996. V. 374. P. 335;  
*Zinov V. G. et al.* JINR Commun. P13-91-182. Dubna, 1991.
16. *Zinov V. G. et al.* // Prib. Techn. Exp. 1998. V. 3. P. 38.
17. *Yukhimchuk A. A. et al.* // Fusion Sci. Techn. 2005. V. 48. P. 294.
18. *Yukhimchuk A. A. et al.* // Hyp. Int. 1998. V. 119. P. 341.
19. *Yukhimchuk A. A. et al.* Preprint VNIIEF 83-2002. Sarov, 2002.
20. *Malkov M. P. et al.* Guide to Physico-Technical Base of Cryogenic. M.: Energoatomizdat, 1973.

21. *Schellenberg L.* // Muon Cat. Fusion. 1990/91. V. 5/6. P. 73;  
Hyp. Int. 1993. V. 82. P. 513.
22. *Gartner B. et al.* // Hyp. Int. 1999. V. 119. P. 103.
23. *Kawamura N. et al.* // Hyp. Int. 1999. V. 118. P. 213;  
*Kawamura N. et al.* // Phys. Lett. B. 1999. V. 465. P. 74.
24. *Demin D.L. et al.* JINR Commun. E15-2003-199. Dubna, 2003.
25. *Adamczak A. et al.* // At. Nucl. Data Tables. 1996. V. 62. P. 255;  
JINR Preprint E4-95-488. Dubna, 1995.
26. *Filchenkov V.V. et al.* // Hyp. Int. 2005. V. 163. P. 143.
27. *Breunlich W.H. et al.* // Phys. Rev. Lett. 1984. V. 53. P. 1137;  
*Breunlich W.H. et al.* // Muon Cat. Fusion. 1987. V. 1. P. 67;  
*Jeitler M. et al.* // Phys. Rev. A. 1995. V. 51. P. 2881.
28. *Bogdanova L.N.* // Muon Cat. Fusion. 1988. V. 3. P. 359.
29. *Hiyama E., Kamimura M.* // RIKEN Rev. 1999. V. 20 P. 34.

Received on July 3, 2008.

Корректор *Т. Е. Попеко*

Подписано в печать 12.11.2008.

Формат 60 × 90/16. Бумага офсетная. Печать офсетная.

Усл. печ. л. 1,18. Уч.-изд. л. 1,67. Тираж 290 экз. Заказ № 56401.

Издательский отдел Объединенного института ядерных исследований  
141980, г. Дубна, Московская обл., ул. Жолио-Кюри, 6.

E-mail: [publish@jinr.ru](mailto:publish@jinr.ru)

[www.jinr.ru/publish/](http://www.jinr.ru/publish/)